INTERNATIONAL JOURNAL FOR NUMERICAL METHODS IN FLUIDS, VOL. 6, 259–274 (1986)

NUMERICAL SOLUTION OF THE ST. VENANT EQUATIONS WITH THE MacCORMACK FINITE-DIFFERENCE SCHEME

REINALDO GARCIA*

Instituto de Mecanica de Fluidos, Universidad Central de Venezuela, Apartado 47762, Caracas 1041-A, Venezuela

AND

RENE A. KAHAWITA*

Hydraulic Departament, Ecole Polytechnique de Montreal, Case Postale 6079 Succ. 'A', Montreal, Quebec H3C 3A7, Canada

SUMMARY

This paper describes the use of the MacCormack explicit time-spilitting scheme in the development of a two-dimensional (in plan) hydraulic simulation model that solves the St. Venant equations. Various tests devised to assess the performance of the method have been performed and the results are reported.

Finally, two industrial applications of the model are presented. The method has been found to be computationally efficient and warrants further development.

KEY WORDS Mathematical Modelling Finite Differences Open Channel Flows St Venant Equations

INTRODUCTION

The use of mathematical models in the simulation of diverse hydraulic phenomena has become essential as a predictive tool in the evaluation of proposed engineering works. Until recently, the engineer was forced to revert to physical modelling in order to simulate, and thereby it was hoped predict, the impact of hydraulic works on the existing river system and its environment. In this last aspect, it is generally accepted that the overall velocity field and the mixing processes are the main factors influencing the water quality in a given system. Mathematical models that calculate the velocity field are therefore of fundamental importance in modern hydraulic engineering practice.

The depth-averaged St. Venant equations describe the motion of water with a free surface and are obtained by integration of the three-dimensional Navier–Stokes equations over the depth, with the assumption of hydrostatic vertical pressure distribution, i.e. negligible vertical accelerations. The need for efficient and accurate numerical schemes to solve these equations is at present of primary concern to computational hydraulics.

In recent years a number of difference schemes have been applied to solve the depth-averaged equations in tidal current flows.[1–3] These schemes use staggered grids, i.e. the velocity components and the water depth are calculated at different points in the numerical grid.

*Assistant Professors

0271–2091/86/050259–16$08.00

Received 26 October 1984
Revised 10 September 1985

Katopodes and Strelkoff[4] presented a solution for the two-dimensional dam-break problem using the method of characteristics.

All these methods seem to be 'problem dependent' in the sense that those schemes well suited for slowly varying flows are not equally efficient for solving rapidly varying flow problems, and vice versa.

The purpose of this article is to report on the results of an investigation into the performance of a mathematical model based on the MacCormack[5] time-splitting scheme when applied to the solution of the two-dimensional shallow water equations. This explicit finite-difference scheme has been successfully applied to solve numerous problems in gas dynamics. It belongs to the class of so-called fractional-step methods, and is second-order accurate in space and time. Moreover, its use in a fully dense grid, where all dependent variables are defined at the same grid point, is expected to reduce the effects of numerical diffusion usually present in first-order schemes.[6]

The main advantage of the proposed method is its ability to simultaneously handle calculations of slowly varying flows as well as rapidly varying flows containing shocks or discontinuities such as those commonly occurring in man-made hydraulic structures.

Various tests performed to assess the accuracy and applicability of the method to typical one- and two-dimensional problems are described. Finally, the solutions of general two-dimensional 'practical' test cases with irregular boundaries and variable bathymetry demonstrate the adaptability of the proposed mathematical model to hydraulic engineering studies.

The high computational efficiency found in the simulation and the results obtained in the tests indicate that the MacCormack scheme could be widely exploited in computational hydraulics.

ST. VENANT SHALLOW WATER EQUATIONS

The St. Venant equations follow from the principles of conservation of mass and momentum as expressed by the three-dimensional Navier–Stokes equations. In large-scale problems, the terms describing the diffusion of momentum due to turbulence are, in general, insignificant compared to the remaining terms in the shallow water equations. The implementation of a sophisticated turbulence model is then generally not considered worth while for such cases. The effects of flow resistance are usually implemented through the use of empirical formulae describing the friction stress with a solid boundary such as the river bed. However, if large-scale circulation is to be simulated, the diffusion of momentum terms have to be present in the equations.[7]

In the present work these terms are included in the equations and the coefficient of turbulent viscosity, or eddy coefficient, will be assumed constant. However, it is important to remark that considering ε constant throughout the flow field ignores the dependence of ε on the velocity, depth and other dynamic parameters that become very important when near-field circulation has to be modelled.

The resulting equations may be written in conservation form as follows.

Conservation of mass equation:

$$\frac{\partial H}{\partial t}+\frac{\partial U}{\partial x}+\frac{\partial V}{\partial y}=0. \tag{1}$$

Conservation of momentum equation in x-direction:

$$\frac{\partial U}{\partial t}+\frac{\partial F}{\partial x}+\frac{\partial G}{\partial y}=E_x. \tag{2}$$

Conservation of momentum equation in y-direction:

$$\frac{\partial V}{\partial t}+\frac{\partial G}{\partial x}+\frac{\partial S}{\partial y}=E_y. \tag{3}$$

Here x and y are horizontal co-ordinates, t is time and the conservation variables are

$$\begin{aligned} H &= h(x, y, t), \\ U &= u(x, y, t)h(x, y, t), \\ V &= v(x, y, t)h(x, y, t), \\ F &= u^2h+\tfrac{1}{2}gh^2, \end{aligned} \tag{4}$$

$$\begin{aligned} G &= uvh, \\ S &= v^2h+\tfrac{1}{2}gh^2. \end{aligned} \tag{5}$$

E_x and E_y are source terms defined as

$$E_x(x, y, t)=gH(S_{0x}-S_{fx})+fV-\frac{1}{\rho}\tau_{sx}+\frac{\partial}{\partial x}\left(\varepsilon\frac{\partial U}{\partial x}\right)+\frac{\partial}{\partial y}\left(\varepsilon\frac{\partial U}{\partial y}\right) \tag{6}$$

and

$$E_y(x, y, t)=gH(S_{0y}-S_{fy})-fU-\frac{1}{\rho}\tau_{sy}+\frac{\partial}{\partial x}\left(\varepsilon\frac{\partial V}{\partial x}\right)+\frac{\partial}{\partial y}\left(\varepsilon\frac{\partial V}{\partial y}\right). \tag{7}$$

In these equations h is the water depth, u, v are depth-averaged velocities in the x- and y-directions, respectively, f is the Coriolis parameter and g is the gravitational acceleration. S_{0x} and S_{0y} are the bottom bed slopes, defined as

$$S_{0x}=-\frac{\partial Z_f}{\partial x}$$

and

$$S_{0y}=-\frac{\partial Z_f}{\partial y}, \tag{8}$$

where Z_f is the bed elevation; S_{fx} and S_{fy} correspond to the bottom friction slopes and, when approximated by the Manning formula and expressed in terms of conservation variables, take the forms

$$S_{fx}=\frac{n^2U(U^2+V^2)^{1/2}}{H^{10/3}} \tag{9}$$

and

$$S_{fy}=\frac{n^2V(U^2+V^2)^{1/2}}{H^{10/3}}, \tag{10}$$

n being the Manning coefficient. τ_{sx} and τ_{sy} are the wind-induced surface stresses, ε is the coefficient of turbulent viscosity, or eddy coefficient, and ρ is the water density, assumed constant.

Equations (1)–(3) constitute a system of quasilinear hyperbolic partial differential equations when $\varepsilon=0$. Practical values of ε used in the computations are small, so that the system is only slightly parabolic in some regions although in the main conserving its hyperbolic character. Therefore this set of equations admits weak solutions, such as surface shock waves with height discontinuities that are commonly observed in practice. The ability to numerically obtain these weak solutions is sometimes of considerable importance in certain engineering applications.

Table I. Required number of boundary conditions at open or 'ocean' boundaries

	Subcritical flow		Supercritical flow	
	Inflow b.c.s	Outflow b.c.s	Inflow b.c.s	Outflow b.c.s
1-D problems	1	1	2	0
2-D problems	2	1	3	0

A consistent set of boundary conditions is required to complete equations (1)–(3). At closed boundaries (e.g. solid walls limiting the flow field) the vanishing of the normal velocity component suffices when $\varepsilon = 0$; however, if $\varepsilon \neq 0$, non-slip boundary conditions must be imposed, i.e. the additional condition of zero tangential velocity at the wall is necessary.

Open or 'ocean' boundaries are those where flow can enter or leave the computational domain. The flow regime (subcritical or supercritical) will determine the correct boundary conditions to be imposed. Stoker,[8] Daubert and Graffe[9] and Verboom *et al.*[10] have studied the mathematical basis for the specification of the boundary conditions for the shallow water equations. They conclude that two-dimensional subcritical flows form a 'well-posed' problem when two boundary conditions (e.g. u and v) are specified at inflow boundaries, whereas only one boundary condition is required at outflow boundaries. Two-dimensional supercritical flows require the imposition of three boundary conditions along inflow boundaries with outflow boundaries remaining 'free' or unspecified. In practice, some numerical condition must be assumed even at a 'free' open boundary owing to the discretization requirements for the derivatives. In this work, zero first derivatives were found to provide satisfactory results. In Table I the minimum numbers of boundary conditions required for the one- and two-dimensional water equations have been summarized.

THE MacCORMACK NUMERICAL SCHEME

The explicit finite-difference method used in this work is based on the MacCormack[5] time-splitting scheme, originally conceived for the solution of the compressible Navier–Stokes equations. The MacCormack scheme is a fractional-step method where a complicated finite-difference operator is 'split' into a sequence of simpler ones. The splitting process reduces the number of calculations during each time step and achieves second-order accuracy in space and time when a symmetric sequence of operators is used.

In order to numerically integrate the shallow water equations the physical continuum region of interest is overlayed with a computational grid where all dependent variables are defined at the cell centres (fully dense grid), these values being taken to represent average cell properties. Most previous two-dimensional models for the shallow water equations use staggered grids in which the dependent variables are defined at different points in the computational cell. Staggered grids usually generate excessive numerical diffusion compared to fully dense schemes, owing to the need to take averages across cell faces. This artificial diffusion can create numerical circulation as well as smearing of shocks or discontinuities. Moreover, fully dense grids are conceptually more consistent than staggered grids.

In the MacCormack time-split scheme, the solution at time $(n+1)\Delta t$, for the computational point (i,j), is obtained by application of

$$U_{i,j}^{n+1} = L_x(\Delta t_x)L_y(\Delta t_y)L_y(\Delta t_y)L_x(\Delta t_x)U_{i,j}^{n}, \tag{11}$$

in which L_x and L_y are one-dimensional finite-difference operators, $U_{i,j}^{n+1} = U(i\Delta x, j\Delta y, (n+1)\Delta t)$,

Δx, Δy and Δt are space and time intervals, respectively, $\Delta t_x = \Delta t_y = \frac{1}{2}\Delta t\ j$, i.e. each operator is advanced by a complete time step.

Each operator in equation (11) is composed of a predictor–corrector sequence. The L_x operator for the shallow water equations may be written as follows.

Predictor sequence (backward differences are used to discretize first-order derivatives):

$$H^{\mathrm{p}}_{i,j} = H^0_{i,j} - \frac{\Delta t_x}{\Delta x}(U^0_{i,j} - U^0_{i-1,j}), \tag{12}$$

$$\begin{aligned} U^{\mathrm{p}}_{i,j} = {} & U^0_{i,j} - \frac{\Delta t_x}{\Delta x}(F^0_{i,j} - F^0_{i-1,j}) \\ & + g\Delta t_x\left(\frac{H^0_{i,j} + H^0_{i-1,j}}{2}\right)\left[-\left(\frac{Z_{\mathrm{f}_{i,j}} - Z_{\mathrm{f}_{i-1,j}}}{\Delta x}\right) - S^0_{\mathrm{f}x_{i,j}}\right] \\ & + \Delta t_x\left(fV^0_{i,j} - \frac{\tau^0_{\mathrm{s}x_{i,j}}}{\rho}\right) + \varepsilon\frac{\Delta t_x}{\Delta x^2}(U^0_{i-1,j} - 2U^0_{i,j} + U^0_{i+1,j}), \end{aligned} \tag{13}$$

$$V^{\mathrm{p}}_{i,j} = V^0_{i,j} - \frac{\Delta t_x}{\Delta x}(G^0_{i,j} - G^0_{i-1,j}) + \varepsilon\frac{\Delta t_x}{\Delta x^2}(V^0_{i-1,j} - 2V^0_{i,j} + V^0_{i+1,j}). \tag{14}$$

Corrector sequence (forward differences):

$$H^{\mathrm{c}}_{i,j} = \frac{1}{2}\left[H^0_{i,j} + H^{\mathrm{p}}_{i,j} - \frac{\Delta t_x}{\Delta x}(U^{\mathrm{p}}_{i+1,j} - U^{\mathrm{p}}_{i,j})\right], \tag{15}$$

$$\begin{aligned} U^{\mathrm{c}}_{i,j} = \frac{1}{2}\Bigg\{ & U^0_{i,j} + U^{\mathrm{p}}_{i,j} - \frac{\Delta t_x}{\Delta x}(F^{\mathrm{p}}_{i+1,j} - F^{\mathrm{p}}_{i,j}) \\ & + g\Delta t_x\left(\frac{H^{\mathrm{p}}_{i+1,j} + H^{\mathrm{p}}_{i,j}}{2}\right)\left[-\left(\frac{Z_{\mathrm{f}_{i+1}} - Z_{\mathrm{f}_{i,j}}}{\Delta x}\right) - S^{\mathrm{p}}_{\mathrm{f}x_{i,j}}\right] \\ & + \Delta t_x\left(fV^{\mathrm{p}}_{i,j} - \frac{\tau^{\mathrm{p}}_{\mathrm{s}x_{i,j}}}{\rho}\right) + \varepsilon\frac{\Delta t_x}{\Delta x^2}(U^{\mathrm{p}}_{i-1,j} - 2U^{\mathrm{p}}_{i,j} + U^{\mathrm{p}}_{i+1,j})\Bigg\}, \end{aligned} \tag{16}$$

$$V^{\mathrm{c}}_{i,j} = \frac{1}{2}\left[V^0_{i,j} + V^{\mathrm{p}}_{i,j} - \frac{\Delta t_x}{\Delta x}(G^{\mathrm{p}}_{i+1,j} - G^{\mathrm{p}}_{i,j}) + \varepsilon\frac{\Delta t_x}{\Delta x^2}(V^{\mathrm{p}}_{i-1,j} - 2V^{\mathrm{p}}_{i,j} + V^{\mathrm{p}}_{i+1,j})\right]. \tag{17}$$

The L_y operator may be written as follows:

Predictor sequence (L_y operator):

$$H^{\mathrm{p}}_{i,j} = H^0_{i,j} - \frac{\Delta t_y}{\Delta y}(V^0_{i,j} - V^0_{i,j-1}), \tag{18}$$

$$U^{\mathrm{p}}_{i,j} = U^0_{i,j} - \frac{\Delta t_y}{\Delta y}(G^0_{i,j} - G^0_{i,j-1}) + \varepsilon\frac{\Delta t_y}{\Delta y^2}(U^0_{i,j-1} - 2U^0_{i,j} + U^0_{i,j+1}), \tag{19}$$

$$\begin{aligned} V^{\mathrm{p}}_{i,j} = {} & V^0_{i,j} - \frac{\Delta t_y}{\Delta y}(S^0_{i,j} - S^0_{i,j-1}) \\ & + g\Delta t_y\left(\frac{H^0_{i,j} + H^0_{i,j-1}}{2}\right)\left[-\left(\frac{Z_{\mathrm{f}_{i,j}} - Z_{\mathrm{f}_{i,j-1}}}{\Delta y}\right) - S^0_{\mathrm{f}y_{i,j}}\right] \\ & + \Delta t_y\left(-fU^0_{i,j} - \frac{\tau^0_{\mathrm{s}y,i,j}}{\rho}\right) + \varepsilon\frac{\Delta t_y}{\Delta y^2}(V^0_{i,j-1} - 2V^0_{i,j} + V^0_{i,j+1}). \end{aligned} \tag{20}$$

Corrector sequence (L_y operator):

$$H^{c}_{i,j}=\frac{1}{2}\left[H^{0}_{i,j}+H^{p}_{i,j}-\frac{\Delta t_y}{\Delta y}(V^{p}_{i,j+1}-V^{p}_{i,j})\right], \tag{21}$$

$$U^{c}_{i,j}=\frac{1}{2}\left[U^{0}_{i,j}+U^{p}_{i,j}-\frac{\Delta t_y}{\Delta y}(G^{p}_{i,j+1}-G^{p}_{i,j})+\varepsilon\frac{\Delta t_y}{\Delta y^2}(U^{p}_{i,j-1}-2U^{p}_{i,j}+U^{p}_{i,j+1})\right], \tag{22}$$

$$\begin{aligned} V^{c}_{i,j}=\frac{1}{2}\Bigg\{ & V^{0}_{i,j}+V^{p}_{i,j}-\frac{\Delta t_y}{\Delta y}(S^{p}_{i,j+1}-S^{p}_{i,j}) \\ & +g\Delta t_y\left(\frac{H^{p}_{i,j+1}+H^{p}_{i,j}}{2}\right)\left[-\left(\frac{Z_{f_{i,j+1}}-Z_{f_{i,j}}}{\Delta y}\right)-S^{p}_{f_{y_{i,j}}}\right] \\ & +\Delta t_y\left(-fU^{p}_{i,j}-\frac{\tau^{p}_{sy_{i,j}}}{\rho}\right)+\varepsilon\frac{\Delta t_y}{\Delta y^2}(V^{p}_{i,j-1}-2V^{p}_{i,j}+V^{p}_{i,j+1})\Bigg\}. \end{aligned} \tag{23}$$

The superscript 0 indicates that results from the previous operator should be used and p indicates that predicted quantities are used to evaluate the conservative variables.

In the L_x operator, the solution is advanced by a time step Δt_x as if the derivatives in the y-direction were absent, and then in the L_y operator by a time step Δt_y omitting the derivatives in the x-direction. Note also that in both operators backward spatial differences are used for the predictor and forward differences for the corrector; however the authors have found, based on extensive numerical experiments, that in equation (11) a cyclic symmetrical discretization of derivatives should be performed in the following manner:

First L_x operator	Predictor: backward differences Corrector: forward differences
First L_y operator	Predictor: backward differences Corrector: forward differences
Second L_y operator	Predictor: forward differences Corrector: backward differences
Second L_x operator	Predictor: forward differences Corrector: backward differences

It is important to remark that, although derivatives are discretized to first-order accuracy, symmetric sequences, such as (11), achieve second-order accuracy in space and time.[5] The stability of the scheme is normally determined by the Courant–Friederichs–Lewy condition; however the particular character of (11) results in a somewhat relaxed criterion, i.e.

$$\Delta t \leqslant \max\left(\frac{2\Delta x}{(u+c)_{\max}}, \frac{2\Delta y}{(v+c)_{\max}}\right).$$

In fact the maximum Courant number ($Cr = \Delta t(u+c)_{\max}/\Delta x$, that guarantees stable results is still $Cr = 1$ for each operator, as in other explicit schemes; however the apparent Courant number of the whole sequence can attain values up to two, and stable results are still obtained, as confirmed by the numerical experiments.

RESULTS AND DISCUSSION

In order to test the general behaviour of the proposed mathematical model, various numerical experiments were performed. One-dimensional elementary problems, to which analytical solutions

exist, were used to verify some fundamental characteristics of the numerical scheme, such as phase and amplitude errors, stability and 'shock-capturing' ability. More complex two-dimensional problems were then attempted to assess the performance of the model and its response to the variation of different parameters involved in the solutions. Finally, general two-dimensional problems with variable bathymetry and irregular boundaries were treated to investigate the adaptability of the mathematical model to industrial applications.

Linear wave

Consider the problem of a linear wave travelling along a horizontal no-friction channel of length L, closed at one end; then the St. Venant equations reduce to

$$\frac{\partial h}{\partial t} + h_0 \frac{\partial u}{\partial x} = 0 \tag{24}$$

and

$$\frac{\partial u}{\partial t} + g \frac{\partial h}{\partial x} = 0, \tag{25}$$

where h_0 is the undisturbed water depth for $t = 0$. Zero flux is imposed at $x = L$ and the inlet boundary condition is

$$h = A \operatorname{sen}(\omega t) + h_0,$$

where A is the wave amplitude and $\omega = 2\pi/T$ is the frequency corresponding to a period T.

For this problem there is an analytical solution given by

$$u_a = -\frac{Ac}{h_0 \cos(\omega L/c)} \operatorname{sen}\left[(\omega L/c)\left(\frac{x}{L} - 1\right)\right] \cos(\omega t), \tag{26}$$

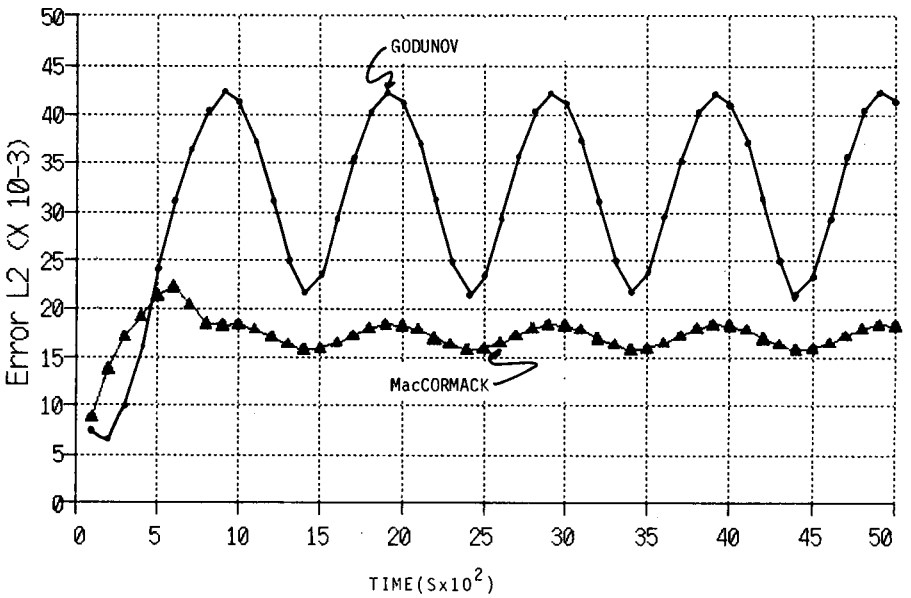

Figure 1. Error L_2 obtained with the MacCormack and Godunov schemes for the linear wave test. $L = 200\,\text{m}$, $A/h_0 = 0{\cdot}025$, $T = 200\,\text{s}$

$$h_a = \frac{A}{\cos(\omega L/c)} \cos\left[(\omega L/c)\left(\frac{x}{L} - 1\right)\right] \operatorname{sen}(\omega t) + h_0. \tag{27}$$

To compare the analytical and numerical solutions use is made of the L_2 error defined as

$$\mathrm{Err}^{L_2} = \left\{ \frac{\sum_i [(u_i^n - u_a)^2 + (h_i^n - h_a)^2]}{\sum_i [(u_i^0)^2 + (h_i^0)^2]} \right\}^{1/2} \tag{28}$$

where the superscript n corresponds to the nth time step and 0 to the initial conditions.

This error measure takes into account the numerical error in u and h for all computational points and for a given time.

Figure 1 shows the time-dependent error obtained with the MacCormack scheme compared with the numerical solution given by the Godunov[11] first-order scheme. Note that for the discretization used the Err^{L_2} never goes over 2 per cent for the MacCormack scheme, whereas the Godunov scheme gives errors arround 4·5 per cent with higher error amplitudes.

This test shows, in the first place, that the MacCormack scheme gives accurate solutions for the linearized St. Venant equations and secondly that it is obviously superior to first-order accurate schemes such as that of Godunov.

Wave amplitude error, phase error and numerical convergence test

This test (similar to the previous one) concerns the modelling of a free oscillation in a rectangular channel, open at its upstream end (inlet) and closed at its downstream end (reflective solid wall) but the full non-linear equations are used. Ideal flow is also assumed. Initially, the water is at rest with uniform depth, $h = h_0$. However in this case the inlet water level is suddenly raised at $t = 0$ to $h = h_0 + \Delta h$ and is held constant thereafter (see Figure 2).

This boundary condition generates a travelling wave, of height Δh, that propagates along the channel. When the wave reaches the solid wall, where zero flux is prescribed, reflection occurs and

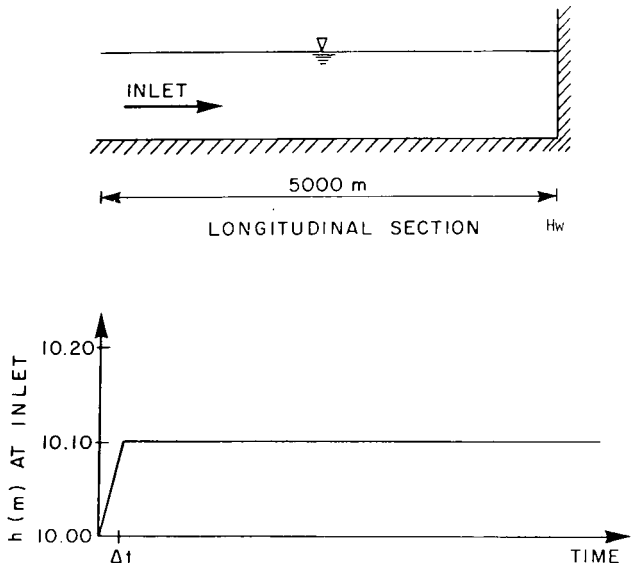

Figure 2. Rectangular channel and boundary conditions at inlet

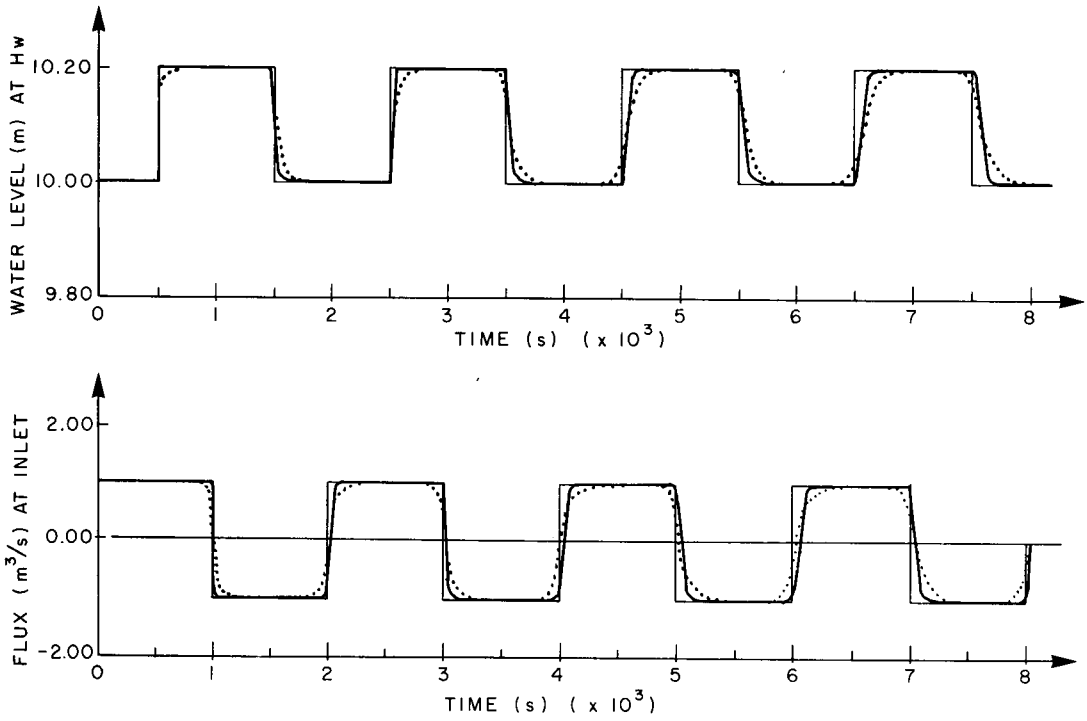

Figure 3. Numerical convergence, amplitude and phase error test:------$x = 250$ m, ——$x = 100$ m.

its height increases to $2\Delta h$. This example is considered an extreme test situation for numerical models.[12]

The numerical model should correctly reproduce the speed of the disturbance ($c = \sqrt{(gh)}$) and its period, T. Also the artificial diffusion introduced by the numerical scheme, mainly due to truncation and discretization errors, should be as low as possible in order to properly represent the wave front. It is also important to test the convergence of the finite-difference approximation in the sense that as Δt and Δx (time and space intervals) tend to zero, the numerical solution should continuously approach the analytical solution.

Figure 3 shows the transient variation of water depth at the computational point closest to the solid wall, Hw, as well as the transient variation of volume flux at the inlet for two test runs. The computed speed ($c = 9{\cdot}9$ m/s) coincides with the analytical value ($c = \sqrt{(gh)}$). No artificial attenuation on damping is found even though a long period of time (8000 s) is simulated. Figure 3 also indicates that the numerical solution tends to the analytical one (which is a step function of period 2000 s) when Δx and Δt are reduced. This, of course, is far from being a rigorous convergence proof but it gives a practical assurance of the consistency of the model when applied to more complex situations.

Figure 4 shows the effect of bottom friction on wave attenuation together with the results obtained from the mathematical model of Meissner[12] based on a finite-element algorithm. It can be seen that meissner's model artificially attenuates the wave although no friction is included in the computation. This reveals that certain numerical solutions may introduce artificial friction and diffusion effects that are completely unrelated to the physical problem under consideration. As seen in Figures 3 and 4 the MacCormack scheme introduces no artificial attenuation even for 'long-term' simulation.

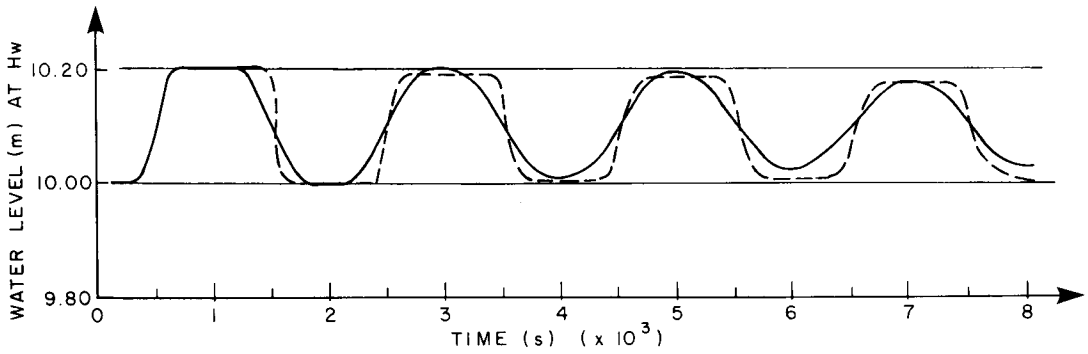

Figure 4. Comparison of MacCormack scheme using $n = 0{\cdot}040$ (---) with the Meissner[12] model using $n = 0{\cdot}0$ (——)

One-dimensional dam-break problem

The one-dimensional 'dam-break' is a test problem in which a vertical wall separating water in a unit-width channel with upstream depth h_1 and downstream depth h_0 ($h_1 > h_0$) is removed instantaneously.

This formulation of the problem is supposed to approximate the flow field resulting from the catastrophic failure of a dam. The flow field consists of a surge wave (depth discontinuity) travelling downstream with speed c_2 and height h_2, while a negative wave with speed c_1 travelling upstream is produced. This sample problem is particularly useful to test the 'shock-capturing' ability of the MacCormack scheme.

The analytical solution to this problem for the case of a straight horizontal channel and frictionless flow may be obtained using the method of characteristics. Figure 5 shows the flow profile for a case where $h_1/h_0 = 16{\cdot}7$.

Table II presents a comparison of computed results with the exact solution for the same case.

In this test, errors are never higher than about 1 percent. Furthermore, tests using extreme water height ratios ($h_1/h_0 = 300$) revealed errors of less than 7 per cent, thus reinforcing the stable properties of the numerical scheme.

Influence of the eddy coefficient, ε, on the circulation pattern

The following test simulates the flow in a sudden expansion in a flat-bed rectangular channel.

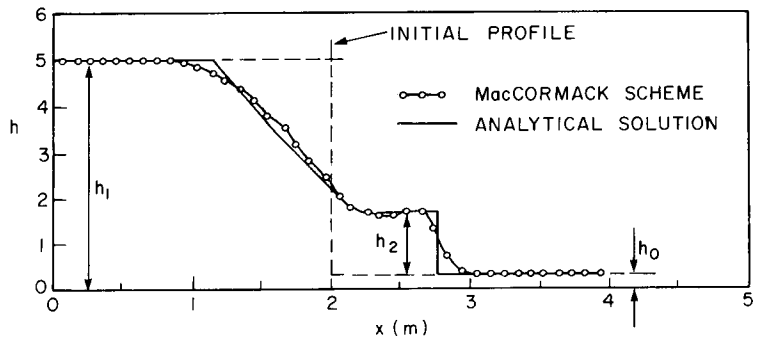

Figure 5. Depth profiles for one-dimensional dam-break test

Table II. Comparison of parameters in dam-break example for $h_1/h_0 = 16{\cdot}7$

	Analytical solution	Numerical solution	Percentage error
Shock speed, c_2	7·3 m/s	7·5 m/s	< 1
Speed of negative wave, c_1	7·0 m/s	6·95 m/s	< 1
Velocity at dam site	4·67 m/s	4·60 m/s	< 1
Depth at dam site	2·22 m	2·29 m	< 1
Maximum height of shock, h_2	1·68	1·70	< 1

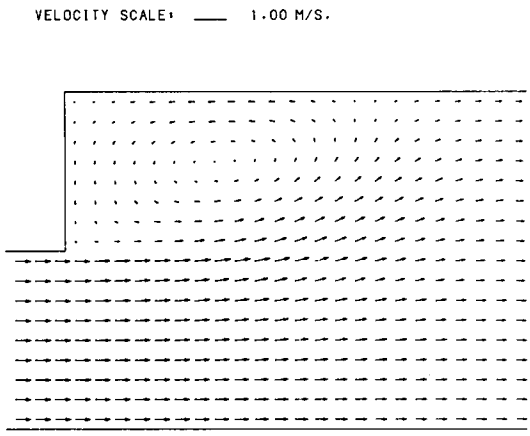

(a)

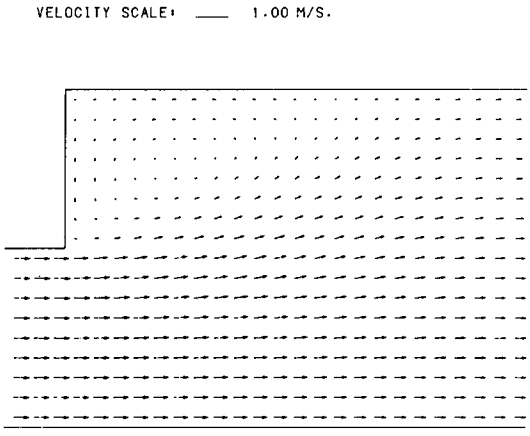

(b)

Figure 6. Sudden expansion test: (a) flow pattern with $\varepsilon = 0{\cdot}1\ m^2/s$; (b) flow pattern with $\varepsilon = 1{\cdot}0\ m^2/s$. For both Figures $\Delta t = 4$ s, $n = 0$, $Q = 100\ m^3/s$

The inerest is to examine the influence of the turbulent diffusion or eddy coefficient, ε, in the circulation pattern.

Figure 6(a) illustrates the steady-state velocity field for $\varepsilon = 0{\cdot}10\,m^2/s$ when a discharge of $Q = 100\,m^3/s$ is imposed at the inlet open boundary.

The results are stable even though the apparent Courant number is approximately 1·9, thus confirming the improved computational efficiency obtained with the introduction of the operator sequence previously described.

Figure 6(b) presents the steady-state velocity field for the same test problem but with a eddy viscosity coefficient ten times large ($\varepsilon = 1{\cdot}0\,m^2/s$) than that used in Figure 6(a). Note that, although results are quite similar in the main flow, the adjacent recirculating eddy has been almost suppressed. This is in accordance with the results obtained by Abbott and Rasmussen.[13] Moreover, numerical experiments show that the eddy coefficient is not required to stabilize the solution.

It is important to note that some mathematical models recently developed include an undesirably high value of the eddy viscosity in order to obtain stable and well-behaved solutions. These models use mainly finite-element algorithms[14] but some finite difference models also evidence this restriction.[2] It is doubtful, therefore, whether such models, that calculate the two-dimensional velocity field, could be used with success in conjunction with expressions for the subgrid scale turbulence, since the viscosities they require are usually many orders of magnitude higher than physically realistic ones; values of $\varepsilon = 50$ (!) are common.[14,15]

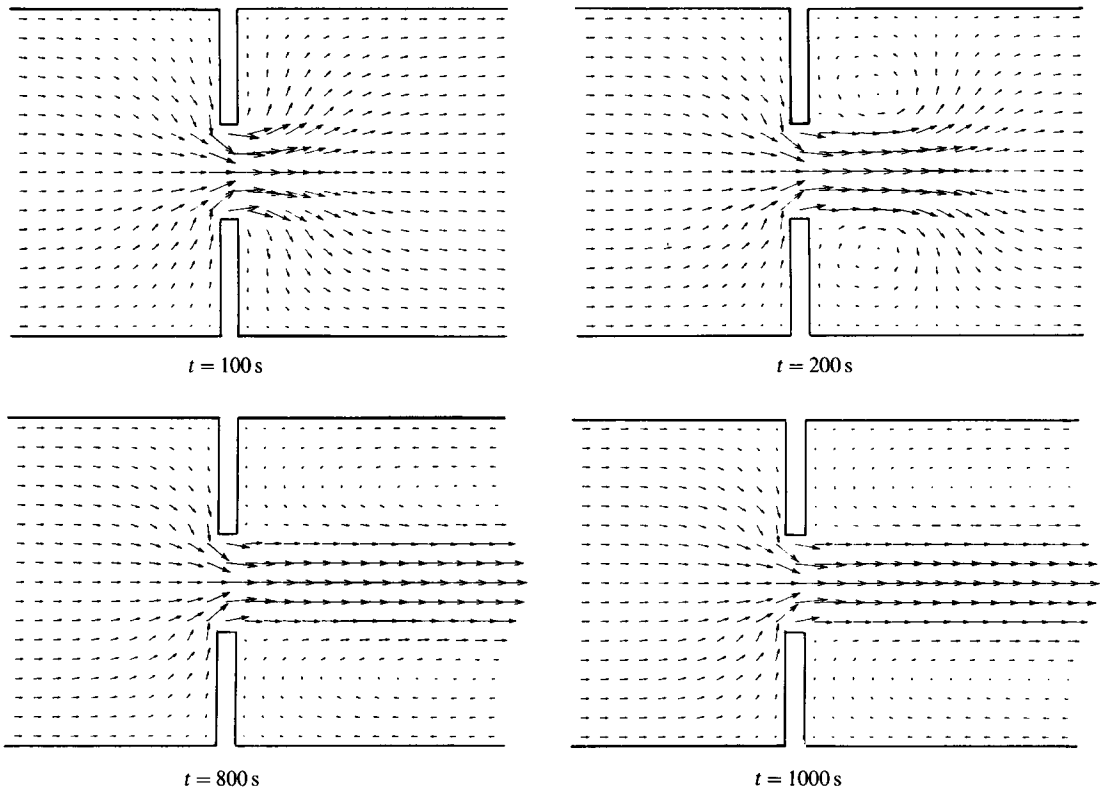

Figure 7. Symmetrical contraction test: flow patterns for $Q = 100\,m^3/s$. $\Delta t = 2{\cdot}5\,s$, $\Delta x = \Delta y = 11\,m$, $n = 0$ and $\varepsilon = 0{\cdot}5$. Velocity scale → 1·00 m/s

Flow through a symmetrical contraction

This problem concerns the simulation of the flow through a symmetrical contraction in a horizontal rectangular channel. The objective is to test the performance of the model in a relatively complex flow situation where the non-linear terms are important due to the rapid convergence and divergence of the velocity field, and where different types of boundaries exist. In the open upstream boundary of the channel, constant discharge as well as zero transverse velocities are imposed. The outflow end is unspecified except for the implicit assumption of zero first derivatives. Initial conditions are zero velocities and a uniform depth of two metres everywhere.

Figure 7 presents a time-frame sequence of the flow field obtained when the discharge Q is $100\,m^3/s$. Non-slip boundary conditions are imposed at solid walls and $\varepsilon = 0{\cdot}5\,m^2/s$. Stable and symmetric results are obtained even though an apparent Courant number greater than one ($Cr = 1{\cdot}25$) is used. In the initial phase the flow converges before passing through the contraction and diverges when it enters the expansion zone, then a circulation zone is generated and starts to move downstream. The vortex so formed is then stretched downstream and the main flow becomes concentrated at the centre. The Figure presents flow patterns up to 1000 s (corresponding to 400 time steps) of simulation by which time the circulation cell has already traversed the downstream boundary. This situation where inflow and outflow simultaneously occur across an open boundary is inaccurate and inconvenient[16] but is included here to illustrate the stability and symmetry of the results.

Industrial applications

The final *raison d'être* of mathematical models, for engineering purposes in any case, lies in their ability to solve 'real-world' problems. The tests presented in the previous sections, although critical from a numerical point of view, are too simplified to constitute models of rivers, lakes or estuaries. The physical phenomena associated with these 'real-world' problems are usually accompanied by great changes in bathymetry and irregular boundaries. Therefore the present problem has been included to indicate the performance of the proposed model in the context of engineering studies. The practical problem concerns the discharge of a turbine tail race into the lower reservoir of a pumped-storage hydro unit. The approximate area of the reservoir is $3{\cdot}8\,km^2$ and depth variations are of the order of 27 m. The physical domain is discretized into square cells of 100 m × 100 m. The irregular boundaries are then approximated as close as this restriction allows. At the inlet the discharge is initially zero, rising to $3400\,m^3/s$ in 30 s and staying constant afterwards. The width of the tail race is approximately 200 m. Initially velocities are zero everywhere. Figure 8 presents a sequence of flow patterns showing the evolution of the flow field.

The initial period represents a wave propagating into the reservoir. At $t = 150$ s the wave starts to reflect on the opposite boundaries and the high velocities there are due to regions of very shallow water. At $t = 200$ s, reflection is evidenced by reversal of the velocity vectors near boundaries. The zone of the reservoir limited by the closed end starts to be filled and potential energy is stored in the form of an increased water stage. At $t = 500$ s the discharge is almost totally diverted to the open boundary on the left-hand side. The last two Figures corresponding to $t = 2500$ s and $t = 3000$ s show little change in the flow field indicating that the steady state has been almost attained. At this point, an important verification may be performed: the mass flux has to be conserved, i.e. if for $t = 3000$ s the steady state has been reached, then the discharge leaving the domain by the outflow boundary should be the same as that entering the domain from the tail-race discharge. By integrating the velocity field at the outflow boundary the discharge obtained was approximately 3 per cent lower than the inlet discharge. This result is considered very good when

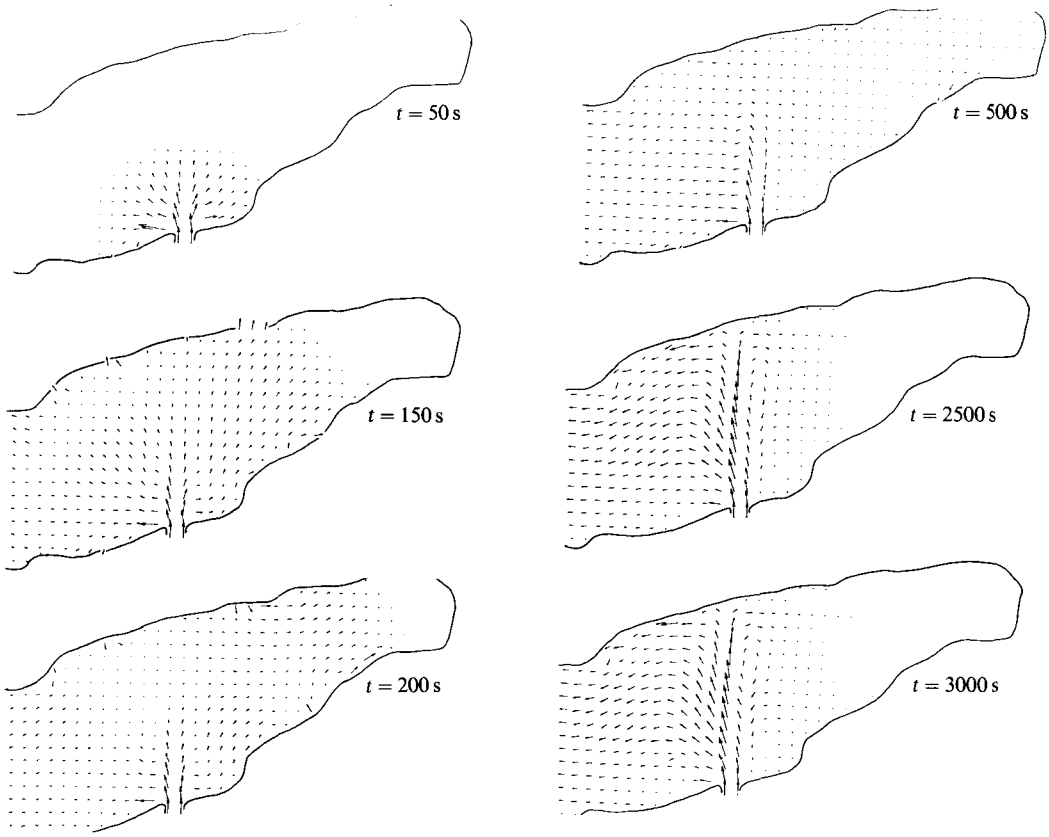

Figure 8. Delaney reservoir: flow patterns. $\Delta t = 10$ s, $\Delta x = \Delta y = 100$ m. (Velocity scale → 1·00 (m/s))

the approximations and discretization errors involved in the computation are considered. The total simulation of this problem took less than 30 s (CPU) on an IBM 3081 computer.

The second practical problem presented concerns the simulation of the flow field in the Lachine rapids: a branch of the St. Laurent river near Montreal. The interest in this problem is to know the steady-state solution for a given set of boundary conditions in order to evaluate the environmental impact of a proposed dam to be constructed on the site. The physical domain was discretized into square cells of 50 m × 50 m. A discharge of 276 m^3/s was specified upstream, and a water elevation of 21·3 m was imposed downstream. Zero initial velocities are assumed. The time step used was five seconds.

This problem is well suited to test the performance of the model, since high velocity gradients occur in the rapids which have to be properly represented in the numerical solution. Figure 9 shows the velocity field for $t = 6000$ s (1200 time steps); at this time the flow has almost reached the steady-state solution. It can be noted that the flow converges towards the contraction near the upstream end. Velocities increase considerably along the contraction where the existing islands affect the flow pattern. Further downstream the flow decelerates. Note that in the narrowing near the downstream end, the velocities increase again. The solution appears to be stable and well behaved everywhere. Good agreement with water stage measurements has been obtained.

The results of these tests show the applicability of the proposed mathematical model to different 'industrial-applications-type' problems, therefore reinforcing the advantages and conveniences of using the MacCormack scheme.

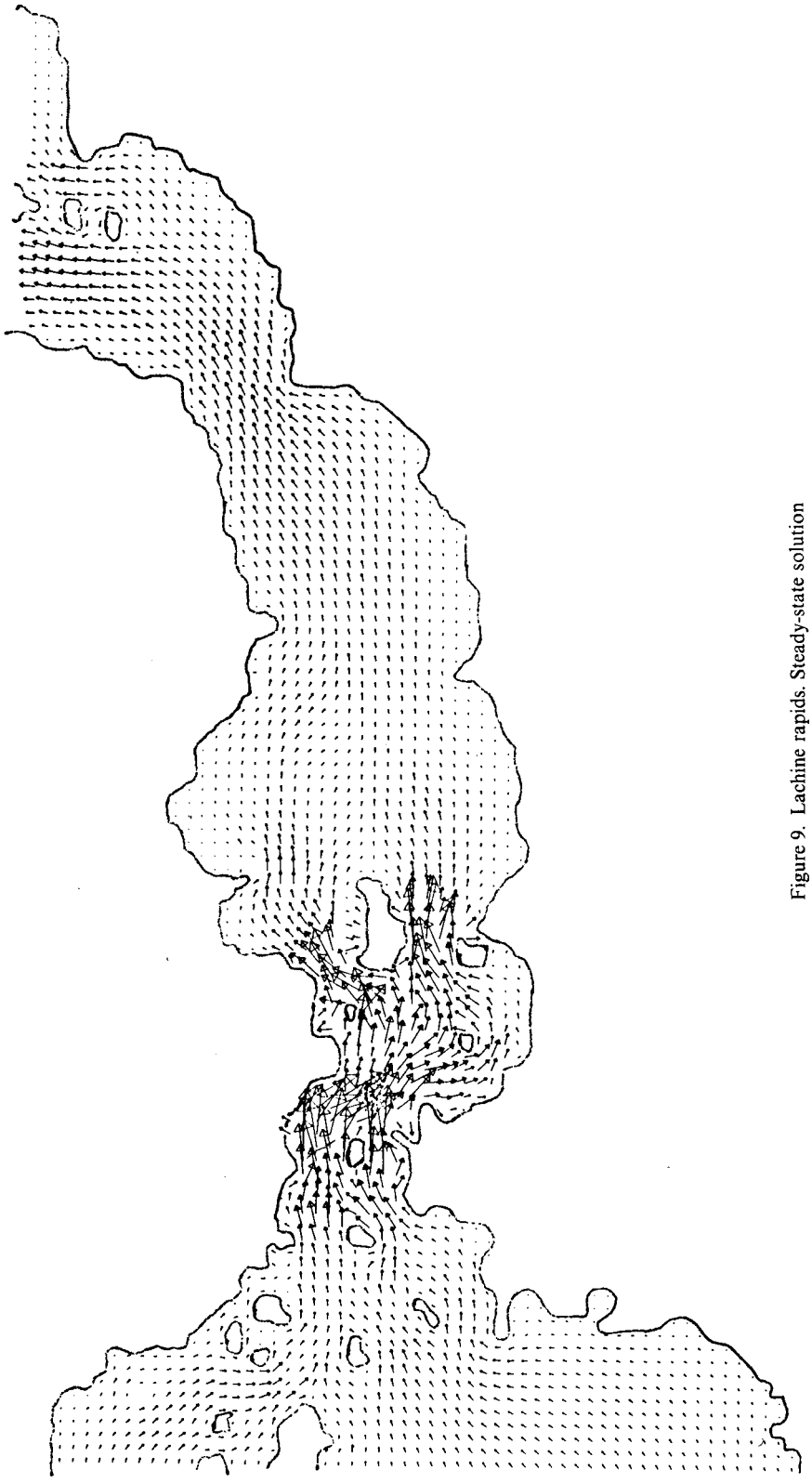

Figure 9. Lachine rapids. Steady-state solution

CONCLUSIONS

This article has described the development of a mathematical model that solves the two-dimensional shallow water equations, based on a version of the explicit MacCormack[5] time-splitting scheme.

The model is able to treat rapidly varying flow problems as well as slowly varying problems that commonly occur in hydraulics.

Verification of the model is made by comparison with one-dimensional analytical solutions and very good agreement has been found. The scheme appears to introduce little numerical viscosity. This has been tested with one- and two-dimensional problems. The two-dimensional tests also show stable and symmetric results for various situations.

A general two-dimensional problem concerning the simulation of a rapidly varying flow fields in an irregular boundary domain is presented to show the performance of the model in 'real-world' or industrial applications. The overall performance of the model is considered very good. Computational costs appear to be small for a model of this type.

REFERENCES

1. R. A. Falconer, 'Numerical modelling of tidal circulation in harbors', *Journal of Waterways. Port, Coastal and Ocean Division, Proc. ASCE*, **106**, 31–48 (1980).
2. V. M. Ponce and S. B. Yabusaki, 'Modeling circulation in depth-averaged flow', *Journal of the Hydraulic Division, Proc. ASCE*, **107**, 1501–1517 (1981).
3. J. P. Benqué, J. A. Cunge, J. Feuillet, A. Hanguel and F. M. Holly, 'New method for tidal current computations', *Journal of the Waterways, Port, Coastal and Ocean Division, Proc. ASCE*, **108**, 396–417 (1982).
4. N. Katopodes and T. Strelkoff, 'Computing two-dimensional dam-break flood waves', *Journal of the Hydraulic Division, Proc. ASCE*, **104**, 1269–1288 (1978).
5. R. W. MacCormack, 'Numerical solution of the interaction of a shock wave with a laminar boundary layer', *Lectures Notes in Physics*, Springer-Verlag, 1971, Vol. 8, pp. 151–163.
6. M. A. Leschziner, 'On the problem of numerical diffusion in first-order finite difference schemes applied to free recirculating flows', *2nd GAMM Conference on Numerical Methods in Fluid Mechanics*, Cologne, 1977.
7. W. Rodi, *Turbulence Models and their Application in Hydraulics*, State-of-The-Art Paper. I.A.H.R., Delft, 1980.
8. J. J. Stoker, *Water Waves*, Interscience Publishers, New York, 1957.
9. A. Daubert and O. Graffe, 'Quelques aspects des écoulements presque horizontaux á deux dimensions en plan et non permanents', *La Houille Blanche*, No. 8, 1967.
10. G. K. Verboom, G. S. Stelling and M. J. Officier, 'Boundary conditions for the shallow water equations', in M. B. Abbott and J. A. Cunge (eds), *Engineering Applications of Computational Hydraulics*, Vol. 1, Pitman, Boston, 1982.
11. S. K. Godunov, 'Difference method for the numerical computation of discontinuous solutions of equations in hydrodynamics', *Mat. Sbornic, N.S.*, **47**, (89), No. 3, 1959.
12. U. Meissner, 'A finite difference-element integration scheme for long-period water wave propagation', *Int. j. numer. methods eng.* **12**, 1161–1169 (1978).
13. M. B. Abbott and C. H. Rasmussen, 'On the numerical modelling of rapid expansions and contractions in models that are two-dimensional in plan', *XVIII Congress of the IAHR*, Baden-Baden, 1972, volume 2.
14. W. G. Gray, 'Do finite-element models simulate surface flow?', *Proc. Third International Conference on Finite Elements in Water Resources*, 1980.
15. J. F. Cochet, G. Dhatt and G. Touzot, 'Comparison of explicit and implicit methods applied to finite-element models of tidal problems', *Third International Conference on Finite Elements in Flow Problems*, 1980.
16. S. V. Patankar, *Numerical Heat Transfer and Fluid Flow*, McGraw Hill, New York, 1980.